Electronic Supplementary Material (ESI) for Journal of Materials Chemistry C.

Supporting Information for

Covalent functionalization of few-layer TiS_2 with tetraphenylporphyrin: toward a donor-acceptor nanohybrid featuring enhanced nonlinear saturation absorption

Yan Fang,[†] *Hui Li,*[†] *Zhiyuan Wei,*[†] *Zihao Guan,*[†] *Naying Shan,*[†] *Lulu Fu,*[†] *Zhipeng Huang,*[†] *Mark G. Humphrey,*[‡] *Chi Zhang*[*, †]

[†] China-Australia Joint Research Center for Functional Molecular Materials, School of Chemical Science and Engineering, Tongji University, Shanghai 200092, China

[‡] Research School of Chemistry, Australian National University, Canberra, ACT 2601, Australia

Section S1. Calculation of nonlinear absorption parameters.

The total absorption coefficient of a material can be written as

$$\alpha(I) = \alpha_0 + \beta I, \qquad \text{(Equation S1)}$$

where α_0 and β are linear absorption coefficient and nonlinear absorption coefficient, respectively. I is the incident light intensity. The corresponding light propagation model is expressed as[1]

$$\frac{dI}{dz} = -\left(\alpha_0 + \beta I\right)I, \qquad \text{(Equation S2)}$$

As for open aperture Z-scan, the normalized transmittance can be given as[1]

$$T(z) = \sum_{m=0}^{\infty} \frac{\left[\frac{-\beta I_0 L_{eff}}{1 + z^2/z_0^2}\right]^m}{(m+1)^{3/2}}, \qquad \text{(Equation S3)}$$

where $L_{eff} = (1 - e^{-\alpha_0 L})/\alpha_0$ is the effective interaction length, α_0 is the linear absorption coefficient, L is the sample thickness, β is the nonlinear absorption coefficient, I_0 is the on-axis peak intensity at the focal plane, and z_0 is the Rayleigh diffraction length.

By fitting the experimental data, the nonlinear absorption coefficient β can be obtained. The imaginary part of the third-order nonlinear susceptibility ($Im\chi^{(3)}$) was calculated according to[2]

$$Im\chi^{(3)} = \left[\frac{10^{-7} C\lambda n^2}{96\pi^2}\right]\beta, \qquad \text{(Equation S4)}$$

where c is the speed of light, λ is the wavelength of the laser, and n is the refractive index.

After transforming the normalized transmittance as a function of laser intensity, we can obtain the saturation intensity (I_s) by fitting the curves with a nonlinear transmission model:[3, 4]

$$T(I) = A * exp\left(\frac{-\Delta T}{1 + I/I_s}\right), \qquad \text{(Equation S5)}$$

where $T(I)$ is the intensity-dependent transmission. ΔT, I_s, and A are modulation depth, saturation intensity, and normalization constant, respectively.

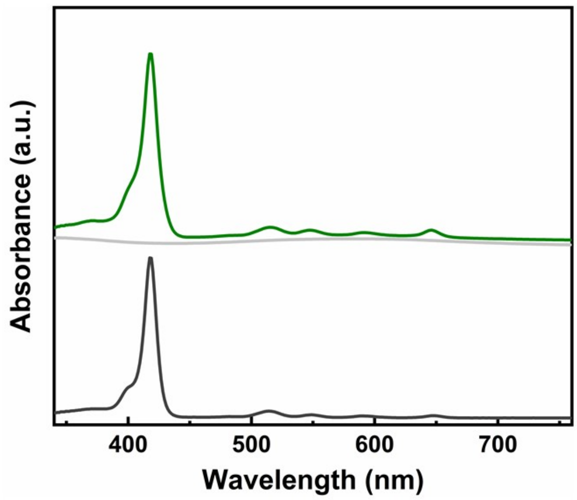

Figure S1. UV-Vis absorption spectra of a mixture containing TPP and exf-TiS_2 (dark grey). Light grey and olive lines represent the isolated solid (the reference sample of physisorbed material) and the filtrate, respectively, after being processed likewise TPP-TiS_2. No absorption peak of TPP could be observed from the light grey line, indicating negligible physisorption.

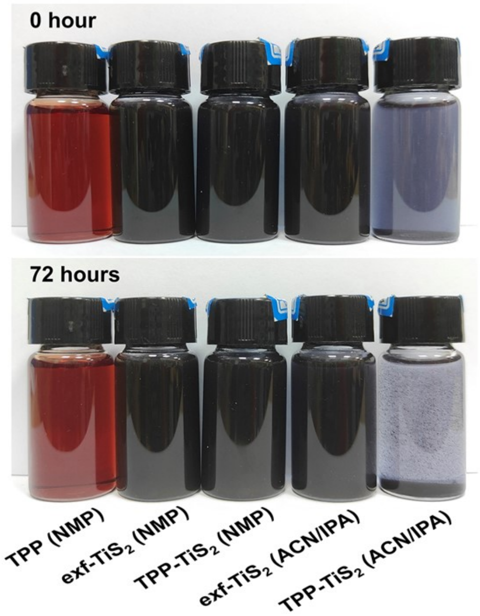

Figure S2. Photographs of TPP, exf-TiS_2, and TPP-TiS_2 dispersions with all concentrations at 0.1 mg ml^{-1}. The top photograph exhibits the fresh dispersions after sonication for 10 minutes; the bottom one shows the dispersions after a 72-hour storage.

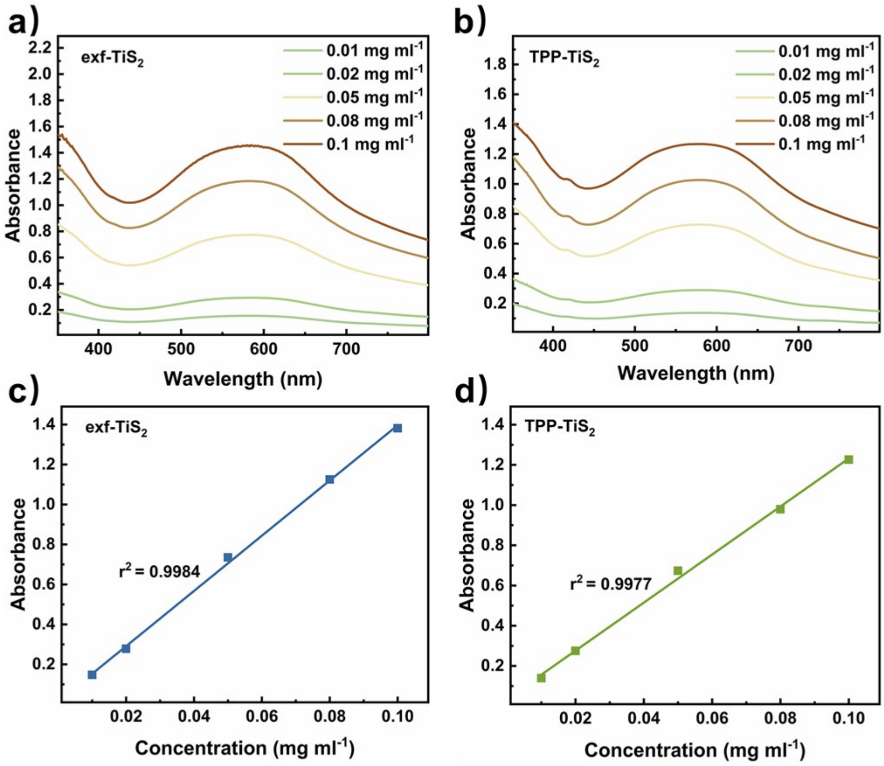

Figure S3. The absorption spectra of NMP dispersions of a) exf-TiS_2, and b) TPP-TiS_2 at different concentration. The optical density of c) exf-TiS_2 and d) TPP-TiS_2 at different concentration at 532 nm.

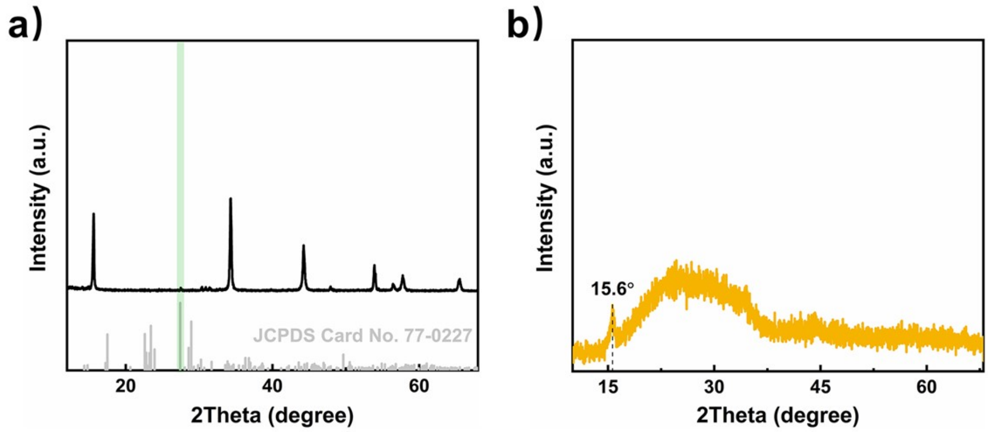

Figure S4. a) XRD pattern of bulk TiS_2 (black) as compared with the standard pattern of S-JCPDS No. 77-0227 (grey). b) XRD pattern of the control sample prepared by treating exf-TiS_2 with the TPP-TiS_2 functionalization process without adding TPP diazonium salts.

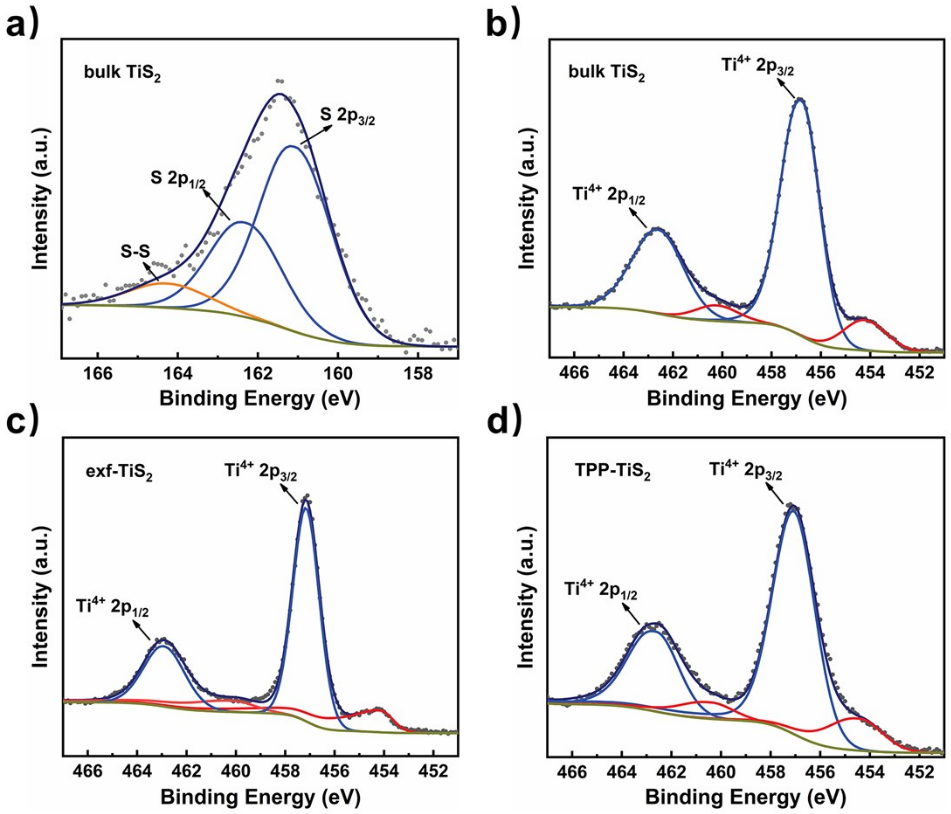

Figure S5. a) S 2p core-level XPS spectrum of bulk TiS_2. Ti 2p core-level XPS spectra of b) bulk TiS_2, c) exf-TiS_2, and d) TPP-TiS_2.

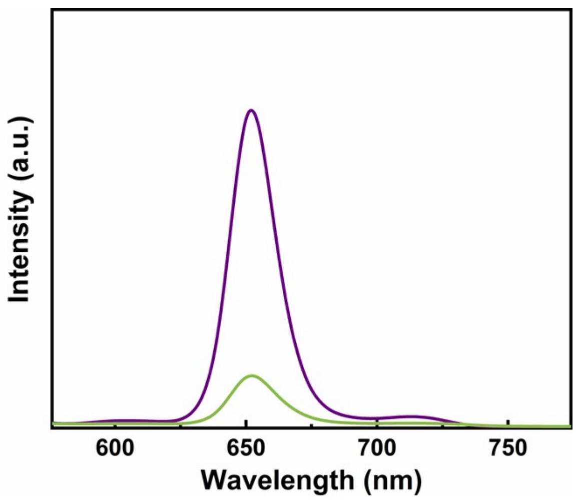

Figure S6. Photoluminescence spectra of TPP (purple) and the physically-blended sample (green) prepared by mixing TPP with exf-TiS_2 in the same content as the TPP-TiS_2 nanohybrid (roughly according to TGA results), obtained in NMP upon excitation at 418 nm.

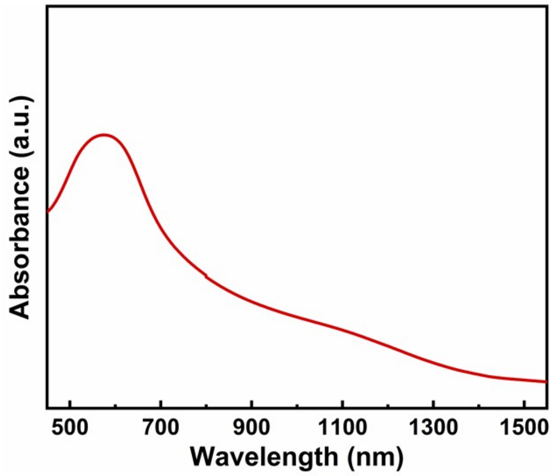

Figure S7. Vis-NIR absorption spectrum of exf-TiS_2 in NMP.

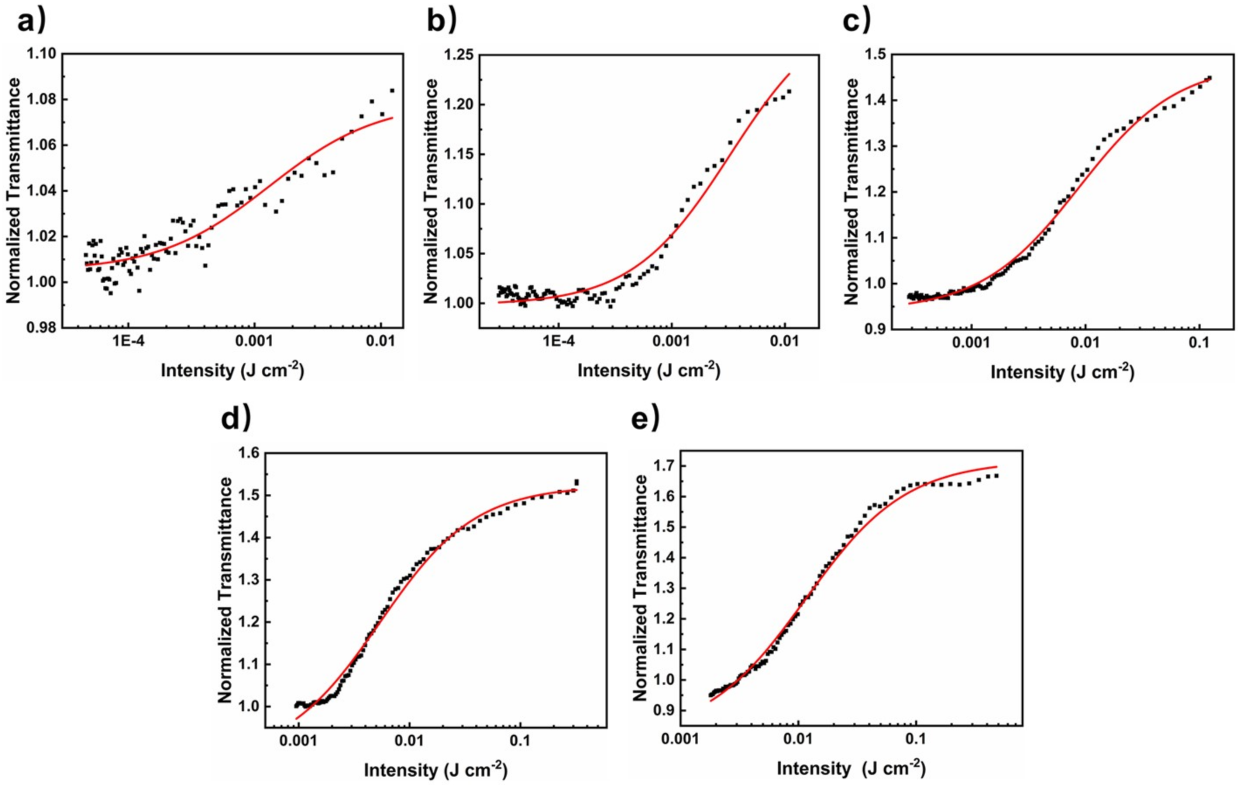

Figure S8. The relationship between normalized transmittance and the laser intensity at pulse energies of a) 6 μJ, b) 14 μJ, c) 42 μJ, d) 110 μJ, and e) 200 μJ, respectively, for exf-TiS_2 at 532 nm.

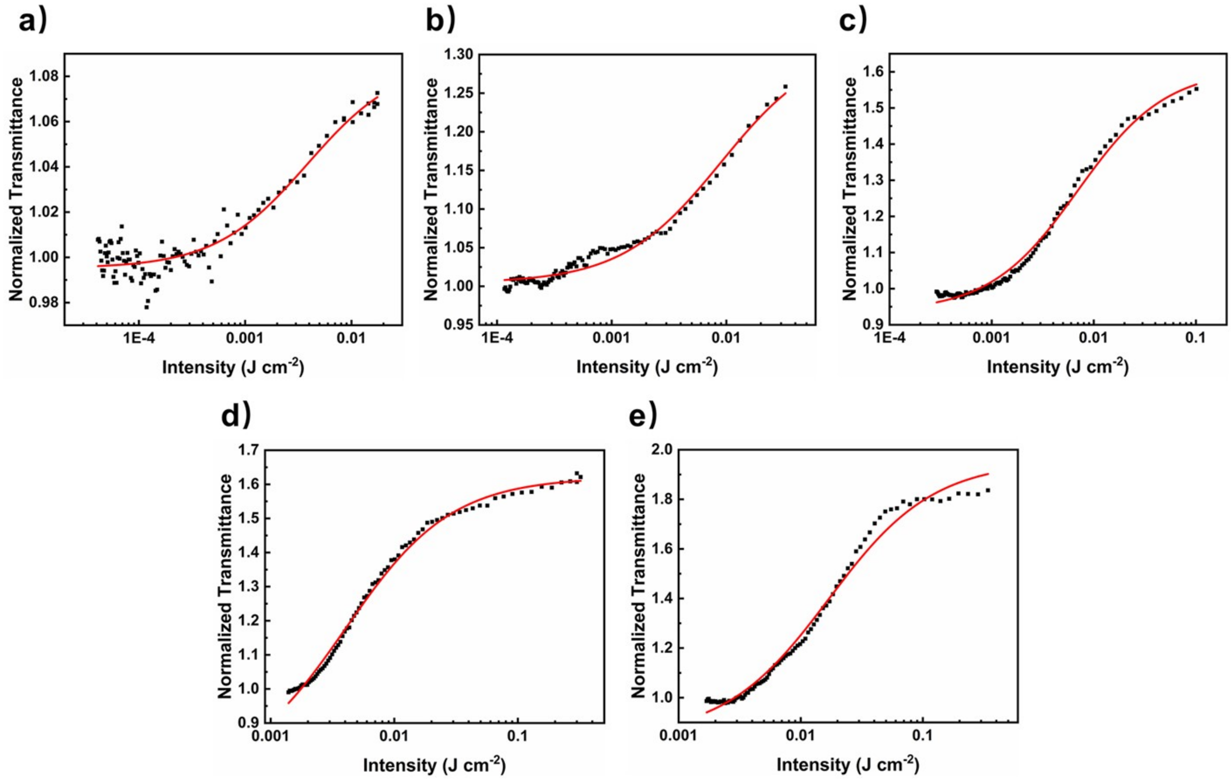

Figure S9. The relationship between normalized transmittance and the laser intensity at pulse energies of a) 6 μJ, b) 16 μJ, c) 42 μJ, d) 110 μJ, and e) 200 μJ, respectively, for TPP-TiS_2 at 532 nm.

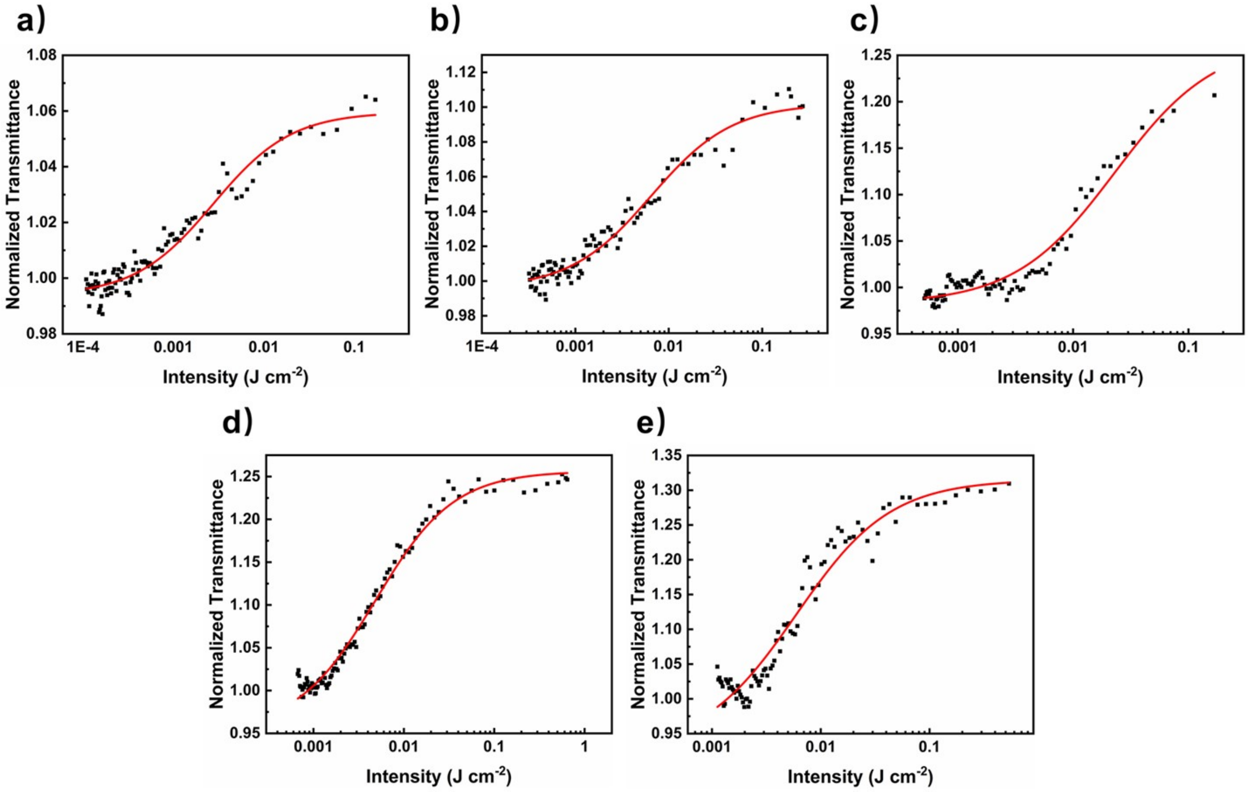

Figure S10. The relationship between normalized transmittance and the laser intensity at pulse energies of a) 60 μJ, b) 92 μJ, c) 132 μJ, d) 220 μJ, and e) 300 μJ, respectively, for exf-TiS_2 at 1064 nm.

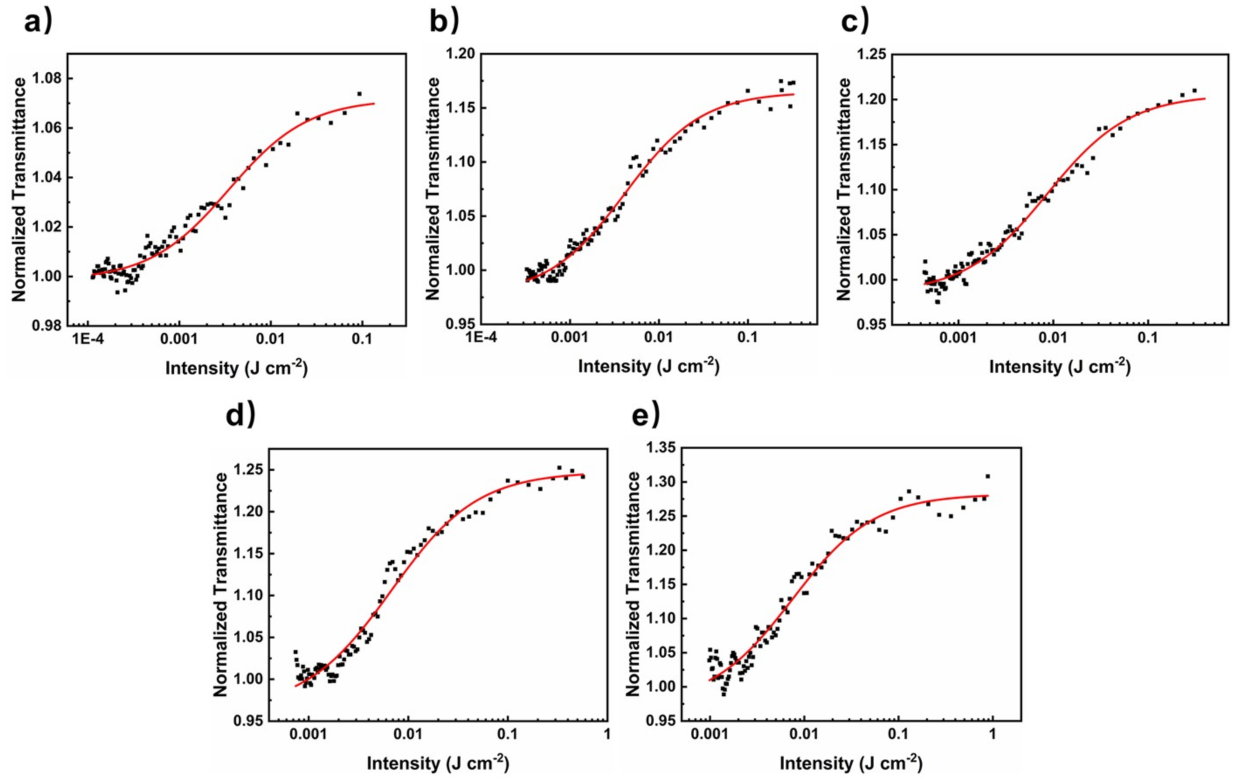

Figure S11. The relationship between normalized transmittance and the laser intensity at pulse energies of a) 60 μJ, b) 100 μJ, c) 151 μJ, d) 220 μJ, and e) 300 μJ, respectively, for TPP-TiS_2 at 1064 nm.

Table S1. Saturation Intensity (I_s) for measured samples under different input fluence at 532 nm and 1064 nm, respectively.[a]

Sample	λ (nm)	E_I (μJ)	I_0 (J cm^{-2})	I_s (J cm^{-2})	Averaged I_s (J cm^{-2})
exf-TiS_2	532	6	0.0177	0.0058	0.0064
		14	0.0413	0.0060	
		42	0.1239	0.0071	
		110	0.3245	0.0053	
		200	0.5900	0.0079	
	1064	60	0.1770	0.0052	0.0053
		92	0.2714	0.0056	
		132	0.3894	0.0057	
		220	0.6490	0.0049	
		300	0.8850	0.0050	
TPP-TiS_2	532	6	0.0177	0.0058	0.0058
		16	0.0472	0.0064	
		42	0.1239	0.0053	
		110	0. 3245	0.0051	
		200	0. 5900	0.0063	
	1064	60	0.1770	0.0050	0.0054
		110	0.3245	0.0046	
		151	0.4455	0.0053	
		220	0.6490	0.0059	
		300	0.8850	0.0061	

[a]λ: the wavelength of incident light; E_I: the energy of the input fluence per pulse; I_0: peak intensity; I_s: saturation intensity.

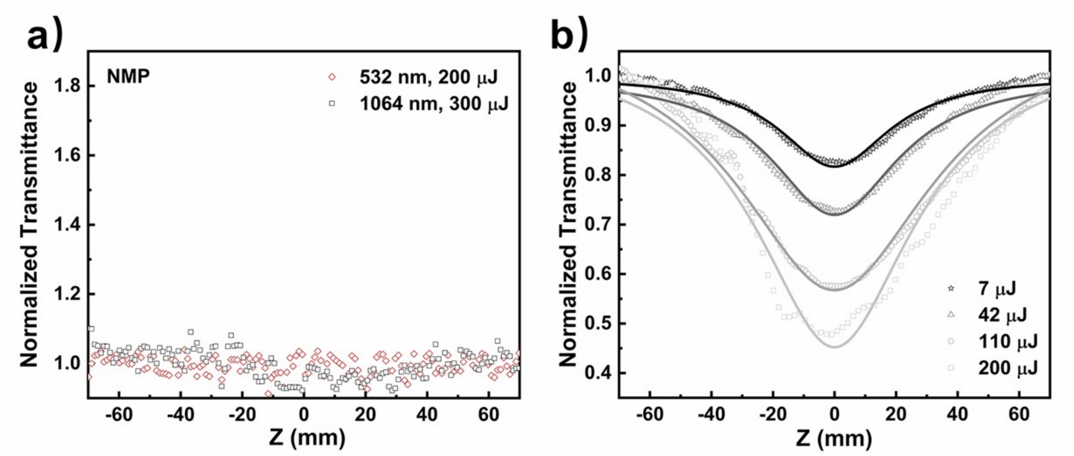

Figure S12. a) Open-aperture Z-scan data of blank solvent NMP at 532 nm under input fluence energy of 200 μJ and 1064 nm under input fluence energy of 300 μJ. b) Open-aperture Z-scan data of TPP solution in NMP under different input fluence energies at 532 nm.

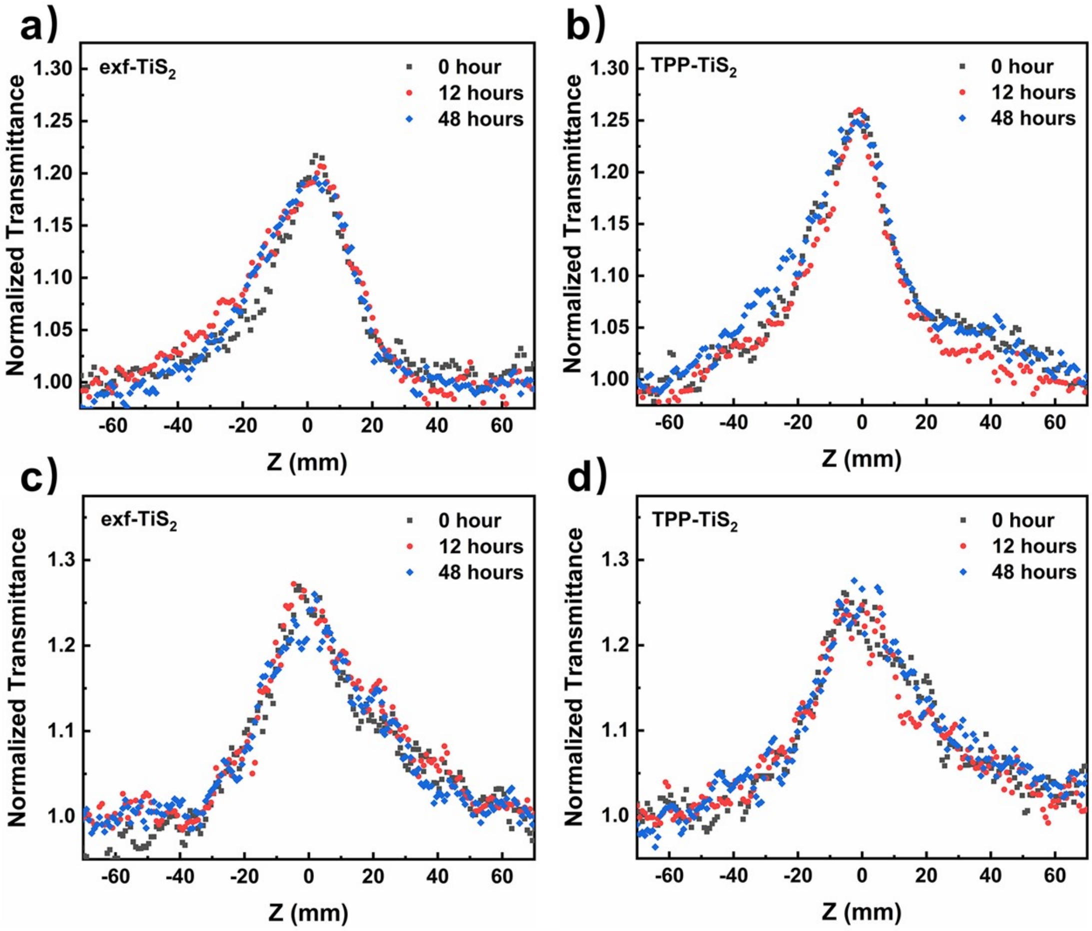

Figure S13. Z-scan results of a) exf-TiS_2 and b) TPP-TiS_2 at 532 nm with 15 μJ pulsed light; c) and d) are Z-scan results of exf-TiS_2 and TPP-TiS_2 at 1064 nm with 200 μJ pulsed light.

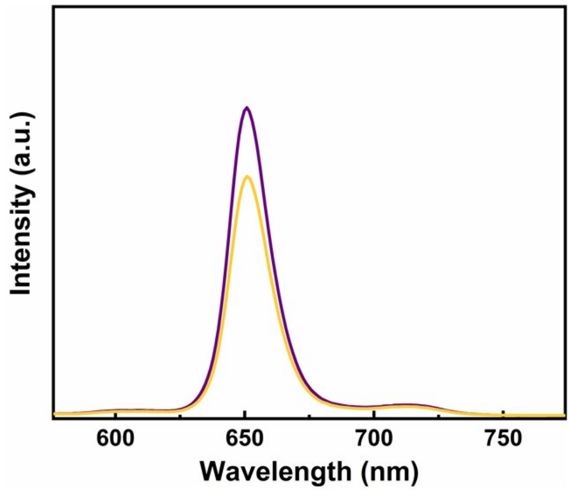

Figure S14. Photoluminescence spectrum of TPP (purple) as compared with the controlling sample TPP/TiS_2, obtained in NMP upon excitation at 418 nm.

References

1 M. Sheikbahae, A. A. Said, T. H. Wei, D. J. Hagan and E. W. Vanstryland, SENSITIVE MEASUREMENT OF OPTICAL NONLINEARITIES USING A SINGLE BEAM, *IEEE Journal of Quantum Electronics*, 1990, **26**, 760-769.

2 H. Li, S. Chen, D. W. Boukhvalov, Z. Yu, M. G. Humphrey, Z. Huang and C. Zhang, Switching the Nonlinear Optical Absorption of Titanium Carbide MXene by Modulation of the Surface Terminations, *ACS Nano*, 2022, **16**, 394-404.

3 H. Yu, H. Zhang, Y. Wang, C. Zhao, B. Wang, S. Wen, H. Zhang and J. Wang, Topological insulator as an optical modulator for pulsed solid-state lasers, *Laser Photonics Rev.*, 2013, **7**, 77-83.

4 S. Wang, H. Yu, H. Zhang, A. Wang, M. Zhao, Y. Chen, L. Mei and J. Wang, Broadband Few-Layer MoS2 Saturable Absorbers, *Adv.Mater*, 2014, **26**, 3538-3544.